

Neutral interstellar hydrogen in the inner heliosphere under influence of wavelength-dependent solar radiation pressure

S. Tarnopolski and M. Bzowski

Space Research Centre, Polish Academy of Sciences, Bartycka 18A, 00-716 Warsaw, Poland
e-mail: slatar@cbk.waw.pl, bzowski@cbk.waw.pl

ABSTRACT

Context. With the plethora of detailed results from heliospheric missions such as Ulysses and SOHO and in advent of the first mission dedicated to in situ studies of neutral heliospheric atoms IBEX we have entered the era of precision heliospheric study. Interpretation of these data require precision modelling, with second-order effects quantitatively taken into account.

Aims. Study the influence of the non-flat shape of the solar Lyman- α line on the distribution of neutral interstellar hydrogen in the inner heliosphere, assess importance of this effect for interpretation of heliospheric measurements.

Methods. Based on available data, construct a model of evolution of the solar Lyman- α line profile with solar activity. Modify existing test-particle code calculating distribution of neutral interstellar hydrogen in the inner heliosphere to take into account the dependence of radiation pressure on radial velocity.

Results. Discrepancies between the classical and Doppler models appear at ~ 10 AU and increase towards the Sun from a few percent to a factor of 2 at 1 AU. The classical model overestimates density everywhere except a $\sim 60^\circ$ cone around the downwind direction, where a density deficit appears. The magnitude of discrepancies depends appreciably on the phase of solar cycle, but only weakly on the parameters of the gas at the termination shock. The intensity of backscatter radiation is weakly affected, as most of the signal comes from regions where the effect is weak, but for in situ measurements of neutral atoms performed at ~ 1 AU, as those planned for IBEX, the Doppler correction will need to be taken into account since the modifications include both the magnitude and direction of the local flux by a few km/s and degree, which, when unaccounted for, would bring an error of a few degrees and a few km/s in determination of the bulk velocity vector at the termination shock.

Conclusions. The Doppler correction is of secondary importance for interpretation of observations of heliospheric Lyman- α glow, but is appreciable for in situ observations of neutral H populations and their derivatives performed at 1 AU.

Key words.

1. Introduction

After discovery at the end of 1960-ties of a diffuse interplanetary Lyman- α glow (Thomas & Krassa 1971; Bertaux & Blamont 1971), predicted by Fahr (1968) and Blum & Fahr (1970) as due to scattering of solar Lyman- α radiation on the neutral interstellar gas flowing through the Solar System, development of models of the distribution of this gas in the heliosphere begun.

At the very early phase, the influence on neutral heliospheric gas of processes going on at the heliospheric interface was neglected. It was assumed that both ionization due to solar output and to radiation pressure acting on the H atoms are stationary and spherically symmetric around the Sun and that they fall off proportionally to inverse square of heliocentric distance. It was further assumed that the inflowing neutral gas is monoenergetic, i.e., that before the encounter with the Sun the atoms move with identical, parallel-oriented velocities. Hence individual velocities of the atoms were adopted as identical with the macroscopic bulk velocity of the gas.

These assumptions formed basis of the first model of density distribution of neutral interstellar gas around the Sun. It was the purely analytic “cold” model (Fahr 1968; Axford 1972). It featured axial symmetry about the axis of inflow of the gas and showed either singularity at the downwind axis when the radiation pressure was too weak to compensate solar gravity, or an

empty “avoidance zone” with a paraboloidal boundary surface when radiation pressure was overcompensating solar gravity.

Lifting of the monoenergetic assumption (allowing for a finite temperature of interstellar gas, high enough to yield thermal velocity comparable to the bulk velocity of the gas), adoption of the distribution function of the gas far away from the Sun (“in infinity”) in the form of Maxwellian shifted in velocity space by the bulk velocity vector, and assumption that the gas is collisionless on the distance scale comparable to the size of the heliosphere allowed to use the Boltzmann equation to describe the problem of interaction of neutral interstellar gas with solar environment. Its solution brought the “hot model” of the gas distribution in the inner heliosphere (Thomas 1978; Fahr 1978, 1979; Wu & Judge 1979). This model required numerical integration of distribution function, but the function itself was still analytic. The “hot model” became the canonical model of neutral interstellar gas distribution in the inner heliosphere.

Further development of modeling of the interaction and distribution of neutral interstellar hydrogen near the Sun focused on two main topics. On one hand, a lot of effort was put to understand and simulate processes going on at the boundary between the expanding solar wind and the incoming partially ionized interstellar gas, in the region referred to as the heliospheric interface – and this issue will not be addressed in the present paper. On the other hand, development of the hot model continued, aimed at a more realistic description of distribution of neutral interstellar hydrogen in the inner heliosphere, suitable for

Send offprint requests to: S. Tarnopolski (e-mail: slatar@cbk.waw.pl)

quantitative, not only qualitative interpretation of heliospheric measurements.

In the first shot, the assumption that the ionization rate is proportional to inverse square of solar distance was eliminated, when Ruciński & Fahr (1989, 1991) realized that the rate of ionization by electron impact does not conform with this simplistic picture. Electron ionization is of particular importance for interstellar helium; for hydrogen it is noticeable inside a few AU from the Sun, where the density of hydrogen gas is already very much reduced by earlier ionization and solar radiation pressure overcompensating solar gravity. Therefore this aspect of physics of neutral interstellar hydrogen was neglected for quite a while since then, but is reintroduced in the most recent versions of the model (Bzowski et al., in preparation).

In the next round of development of the density model, gone was the assumption of invariability of radiation pressure and ionization rate (Ruciński & Bzowski 1995a; Bzowski & Ruciński 1995a,b; Bzowski et al. 1997). Indeed, both the solar EUV flux and the solar wind flux vary considerably during the solar cycle. The result is a solar cycle variation of the solar radiation pressure, of the EUV ionization rate, and of the rate of charge exchange between neutral H atoms and solar wind protons. This in turn results in appreciable variations of density and bulk velocity of neutral interstellar hydrogen within a dozen AU from the Sun.

The new time dependent model was fully numerical because not only the integration of the distribution function had to be performed numerically, as in the “hot model”, but so had to be carried out the calculation of distribution function itself. At this phase of heliospheric research, in lack of sufficiently long time series of measurements of solar wind speed and density and of the solar EUV output substitute, idealized models of evolution of these parameters had to be used.

These aspects of development of the model were discussed in greater detail in a review by Ruciński & Bzowski (1996).

In the next move, effects of interaction of the solar wind and interstellar gas in the heliospheric interface were taken into account. Owing to the charge exchange between the atoms of interstellar gas and the heated and compressed plasma in front of the heliopause, the original population of neutral atoms is somewhat cooled and accelerated, and a new population of atoms appears. These new neutral atoms originally inherit the properties of the parent plasma population, but further decouple from this plasma and flow through the heliopause and inside the termination shock of the solar winds. Both populations interact further with the ionized components, exchanging charge with protons from local plasma. Hence, the processes in the heliospheric interface create a few distinct, collisionless populations of neutral atoms (Baranov et al. (1991); Baranov & Malama (1993), as discussed in detail by Izmodenov (2000) and Malama et al. (2006)).

From the view point of modeling of distribution of neutral interstellar hydrogen in the inner heliosphere, the most important aspect of the processes going on in the heliospheric interface is the modification of distribution function at TS. Instead of the shifted Maxwellian with parameters homogeneous in space, Scherer et al. (1999) adopted a sum of two Maxwellians, with non-isotropic temperatures, shifted by appropriate bulk velocity vectors. The two components of the new functions had parameters being functions of the offset angle θ from the upwind direction and corresponded to the two thermal populations (primary and secondary) as predicted by the Moscow Monte Carlo simulation of heliospheric interface. The model was time dependent, but still axially symmetric. At this time, enough measurements had been published to attempt to introduce observations-based

models of radiation pressure and ionization rate to the simulations.

Axial symmetry was removed in the next round of model development, when anisotropy of the ionization rate was introduced. Bzowski et al. (2001, 2002) allowed the ionization rate to change as function of heliographic latitude, with the latitudinal profile of the ionization rate changing with the phase of solar cycle. Hence the ionization field in the model became 2D (keeping the axial symmetry about the solar rotation axis), and since the gas inflow axis and solar rotation axis are inclined at an angle to each other, the model of neutral hydrogen distribution in the inner heliosphere became 3D and time dependent.

The most recent extension of the model is presented in this paper. We improve on the modeling of radiation pressure acting on individual H atoms, which now is not only a function of time, but also of radial velocity of the atom. In the previous versions of the model it was assumed that the profile of the solar Lyman- α line, responsible for the radiation pressure, is flat. In reality it not only is non-flat, but shows considerable variations depending on the phase of solar activity.

We take this into account and develop an observation-based model of evolution of the line profile as function of line- and disk-integrated flux. We use this model in a newly-developed code which simulates density and higher moments of distribution function of neutral interstellar hydrogen in the inner heliosphere. With the use of the newly-developed code, we assess modifications of the local gas density, of its local flux, and of fluxes of derivative populations with respect to the results of models neglecting the Doppler character of dynamics of neutral interstellar H atoms. We also assess the impact of the new development on simulations of the helioglow and show possible implications for interpretation of heliospheric measurements, both past and planned, including helioglow observations and in situ PUI and neutral atom measurements.

2. The Doppler model of neutral hydrogen distribution in the inner heliosphere

The approach exercised in the present model is a modification of the approach presented by Ruciński & Bzowski (1995a). Density and higher moments of distribution function of neutral interstellar hydrogen at a location \mathbf{R} in the inner heliosphere at a time τ are calculated by numerical integration of the local distribution function constructed as a product of the distribution function in the source region w_{src} and of the probability w_{ion} of survival of the atoms traveling from the source region to the local point against ionization:

$$f(\mathbf{R}, \mathbf{V}, \tau) = w_{\text{src}}(\mathbf{r}_{\text{src}}(\mathbf{R}, \mathbf{V}, \tau), \mathbf{v}_{\text{src}}(\mathbf{R}, \mathbf{V}, \tau)) w_{\text{ion}}(\mathbf{R}, \mathbf{V}, \tau) \quad (1)$$

where $\mathbf{r}_{\text{src}}(\mathbf{R}, \mathbf{V}, \tau)$ is the start position in the source region of the atom that at the local point \mathbf{R} at time τ has velocity \mathbf{V} , and $\mathbf{v}_{\text{src}}(\mathbf{R}, \mathbf{V}, \tau)$ is relevant start velocity in the source region.

The distribution function at the source region w_{src} a priori can be any reasonable function. In the following we adopted it either as a Maxwellian shifted by the bulk velocity vector, homogeneous in space and independent of time:

$$w_{\text{src}}(\mathbf{r}_{\text{src}}, \mathbf{v}_{\text{src}}) = n_{\text{src}} \left(\frac{m}{2\pi k T_{\text{src}}} \right)^{3/2} \exp \left(- \frac{m(\mathbf{v}_B - \mathbf{v}_{\text{src}})^2}{2k T_{\text{src}}} \right) \quad (2)$$

or, in the two-populations case, as a sum of two such functions with different parameters n_{src} (density in the source region), \mathbf{v}_B (bulk velocity at the source region), and T_{src} (temperature at the

source region); m is the atom mass, and k the Boltzmann constant.

The challenging issue in the problem is to find the link between the local velocity of the test atom \mathbf{V} at time τ and location \mathbf{R} and its position \mathbf{r}_{src} and velocity \mathbf{v}_{src} in the source region in the scenario where the force acting on the atom is composed of the attracting solar gravity and the repelling radiation pressure, which is a function of time-varying radiation flux and of radial velocity of the atom. Since both the solar radiation flux and solar gravity fall off with heliocentric distance as $1/r^2$, the radiation pressure can be expressed by the factor μ of compensation of solar gravity. Because the solar Lyman- α flux is a function of time and since the radiation pressure acting on an individual atom owing to the Doppler effect is a function of its radial velocity with respect to the Sun, the μ factor is a function of time and radial velocity: $\mu = \mu(v_r, t)$.

The link between the local position and velocity vectors and the corresponding position and velocity vectors at the source region is determined by numerical solving of the equation of motion specified in Eq.(3), performed backwards in time. Along with the calculation of the trajectory of the atom, its probability of survival is calculated.

$$\frac{d}{dt} \begin{pmatrix} x \\ y \\ z \\ v_x \\ v_y \\ v_z \\ u \\ u_\beta \end{pmatrix} = \begin{pmatrix} v_x \\ v_y \\ v_z \\ -\frac{GM(1-\mu(t,v_r))}{r^3}x \\ -\frac{GM(1-\mu(t,v_r))}{r^3}y \\ -\frac{GM(1-\mu(t,v_r))}{r^3}z \\ \frac{1}{r^2} \\ u\beta_0(r, t, \phi) \end{pmatrix} \quad (3)$$

In the equation above, $\beta_0(r, t, \phi) = r^2 \beta(r, t, \phi)$ is the scaled ionization rate at heliographic latitude ϕ , $r^2 = x^2 + y^2 + z^2$, GM is solar mass times constant of gravity, and $v_r(t) = (\mathbf{r}(t) \cdot \mathbf{v}(t))/|\mathbf{r}(t)|$ is radial velocity of the atom. The position vector $\mathbf{r}(t)$ has coordinates x, y, z and velocity vector $\mathbf{v}(t)$ coordinates v_x, v_y, v_z ; u_β is used to calculate the survival probability as

$$w_{\text{ion}} = \exp(-u_\beta) \quad (4)$$

Once the position and velocity vectors of the test atom in the source region are found, the value of distribution function in the source region can be calculated and after its multiplication with the survival probability w_{ion} the value of the local distribution function can be obtained. To obtain density and higher moments, the local distribution function is numerally integrated in the velocity space.

This scheme is suitable for calculating density distribution in the case of a fully 3D and time dependent radiation pressure and ionization rate. In the present study it was restricted to the spherically symmetric and stationary case.

The model of radiation pressure was developed based on a series of observations of the solar Lyman- α line profiles, performed by SUMER/SOHO between solar minimum and maximum (Lemaire et al. 2002) and available on the Web. It enables to calculate the force of radiation pressure acting on a H atom traveling at radial speed v_r with respect to the Sun, when the disk- and line-integrated solar flux has value I_{tot} . The force is expressed as a compensation factor μ of the solar gravity force.

Since the SUMER instrument is located at the SOHO spacecraft orbiting around the L1 Lagrange point between the Earth and the Sun (Wilhelm et al. 1999), the observations are free from geocoronal contamination that affected earlier measurements

carried out from low-Earth orbits (e.g. OSO-5, Vidal-Madjar 1975). The absolute calibration of the wavelength reported by Lemaire et al. (2002) is better than ± 0.0015 nm. The calibration of intensity was performed by direct comparison of the line-integrated profiles with the line-integrated fluxes obtained with the use of SOLSTICE experiment. The accuracy of the net flux is reported at $\pm 10\%$ level. It seems that the data published on the Web are a smoothed version of actual measurements because despite declared 10% accuracy they do not show any scatter.

To develop the model discussed in this paper, the original data were rescaled to the spectral flux in the μ units and radial velocities in km/s. Fitting to the data the functional forms of the profiles used in earlier studies (Fahr 1978; Chabrilat & Kockarts 1997, H. Scherer, private comm.) did not yield sufficient accuracy of the model (cf Fig. 1 and 2). A satisfactory result could only be obtained with a 12-parameter function in the form:

$$\mu(v_r, I_{\text{tot}}) = (A + B\mu_{\text{tot}}) \left(\exp(-Cv_r^2) (D + E \exp(-Fv_r - Gv_r^2)) \right) + H \exp(-Pv_r - Qv_r^2) \quad (5)$$

with the following parameters:

$$\begin{aligned} A &= 0.2991186310295671 \\ B &= 0.00013667900042797955 \\ C &= 0.000038311829570269574 \\ D &= 8.205079987483719 \times 10^{-9} \\ E &= 6.0618423098629444 \times 10^{-9} \\ F &= 0.04039591137581422 \\ G &= 0.000351354721862217275 \\ H &= 3.9234489096957165 \times 10^{-9} \\ P &= 0.046840910793356665 \\ Q &= 0.0003337345353529254274 \end{aligned}$$

The function (5) with these parameters reproduced well the observed profiles both for solar minimum (the profiles from July 27, 1996 to August 24, 1997) and for solar maximum (the profiles from August 20, 1999 to August 22, 2001) and the accuracy of the fit for the most interesting region ± 140 km/s about the line center exceeds the declared accuracy of the observations. Furthermore, the line-integrated fluxes obtained from the model profiles agree with the line-integrated data and with the total fluxes reported by Tobiska et al. (2000) for a given day. The differences are on the order of 5%; only for the profile observed on May 20, 2000 the difference is 9%, which agrees with the absolute calibration accuracy of 10%. A comparison of the experimental data with the fitted model is shown in Fig. 1.

A comparison of the results of the new model of evolution of the solar Lyman- α line profile with earlier models (Fahr et al. (1981); Chabrilat & Kockarts (1997), H. Scherer, private communication) is presented in Fig. 2.

As the absolute calibration of the line-integrated flux of the Sun changed since the time of publication, we show the original profiles recalibrated by multiplication by appropriate factor so that their absolute flux is in agreement with the values accepted nowadays. The differences between the models in the velocity range ± 100 km/s around the line center are on the order of 10 to 15%. For higher velocities the differences between the models are not so important because atoms that fast are not very sensitive to radiation pressure in general, and the radiation pressure for these atoms is much smaller than for the atoms sitting close to the line center. The highest differences in the absolute terms occur at the peaks of the profile, i.e., at the velocities characteristic for the fast wing of the distribution function of thermal populations of neutral hydrogen in the inner heliosphere. With as many as 9 data sets available, covering the whole span of solar activity

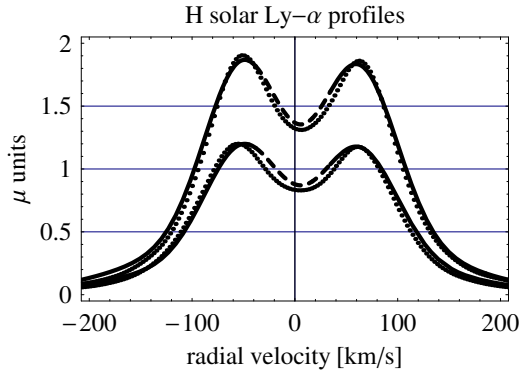


Fig. 1. Selected profiles of the solar Lyman- α line observed by SUMER/SOHO (dots) for solar minimum (lower line, Feb. 17, 1997) and solar maximum (upper line, May 20, 2000), compared with the results of the fitted model, specified in Eq. (5) (lines). The broken part of the model lines is the bulk velocity of the gas in the Local Interstellar Cloud ± 3 thermal speeds of the gas and illustrates the range on the profile which is most relevant for the thermal populations of neutral H atoms in the heliosphere.

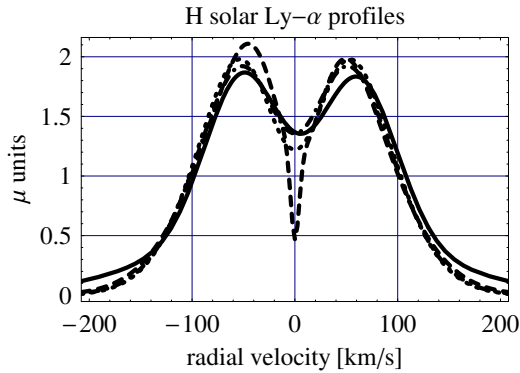


Fig. 2. Comparison of models of solar Lyman- α line profiles: solid line: the present model, dashed line: Chabrilat & Kockart, dashed-dot line: Fahr et al.; dots: Scherer.

level, we were able to come up with a model that seems to better reproduce physical reality than the former ones. Simple multiplicative scaling of the profiles characteristic for one level of solar activity by a factor safeguarding a fit of the line-integrated flux to the measurements performed in a different phase of solar activity does not yield satisfactory results.

3. Calculations

The calculations were performed on a mesh of heliocentric distances r equal to 0.4, 0.7, 1, 2, 4, 7, 10, 20, 50, and 100 AU and offset angles from the upwind directions θ equal to 0° , 30° , 60° , 90° , 120° , 150° , and 180° , separately for solar minimum and solar maximum conditions, characterized by the following values of the line-integrated solar Lyman- α flux and net ionization rate: solar max.: $I_{\text{tot}}=5.50 \times 10^{11}$ photons $\text{cm}^{-2} \text{s}^{-1}$, $\beta = 8 \times 10^{-7} \text{ s}^{-1}$ solar min.: $I_{\text{tot}}=3.53 \times 10^{11}$ photons $\text{cm}^{-2} \text{s}^{-1}$, $\beta = 5 \times 10^{-7} \text{ s}^{-1}$.

In the one-population study, the calculations were performed assuming the temperature at the termination shock 12500 K and bulk velocity 22 km/s, unless otherwise stated in selected cases. In this section by the classical model we mean the hot model as presented, e.g., by Wu & Judge (1979), with the ionization rate falling off as $1/r^2$.

In the two-population simulations discussed in a farther part of the paper we used as boundary conditions at the termination shock the parameters that are returned by the Moscow MC model for the currently preferred set of LIC conditions (Izmodenov et al. 2003):

Primary: $n_{\text{TS,pri}}=0.03465 \text{ cm}^{-3}$, $v_{\text{TS,pri}}=28.512 \text{ km/s}$, $T_{\text{TS,pri}}=6020 \text{ K}$;

Secondary: $n_{\text{TS,sec}}=0.06021 \text{ cm}^{-3}$, $v_{\text{TS,sec}}=18.744 \text{ km/s}$, $T_{\text{TS,sec}}=16300 \text{ K}$,

which were obtained for the interstellar proton and H atoms densities $n_{p,\text{LIC}}=0.06 \text{ cm}^{-3}$, $n_{H,\text{LIC}}=0.18 \text{ cm}^{-3}$, temperature of the gas $T_{\text{LIC}}=6400 \text{ K}$, and bulk velocity $v_{B,\text{LIC}}=26.4 \text{ km/s}$.

To add reality, in this section we introduce electron ionization to both models, classical and Doppler. Details of the electron ionization model used are discussed by Bzowski et al. (2007, in preparation). Since electron ionization was identical in both models, it does not affect the conclusions on the role of wavelength-dependence of radiation pressure, but adds reality to the numerical values of results. The numerical accuracy of the solutions is at the level of 1 to 2%.

4. Results

Discussion of results is split into two parts. In the first one, we will show the influence of the wavelength-dependence of radiation pressure on density and flux of neutral interstellar hydrogen gas in the inner heliosphere as function of such parameters as bulk velocity and temperature in the source region, the ionization rate etc. The basis for the comparison will be results of the classical hot model. In the second part, we will assess the differences between the classical hot model and the present model of density, local bulk velocity and flux of the interstellar hydrogen gas, as well as of the intensities of the backscatter glow and fluxes of the derivative PUI population in the case of a composite gas distribution built up from a sum of the primary and secondary populations of neutral hydrogen atoms, predicted by kinetic models of the heliosphere for the currently favored values of interstellar gas parameters.

4.1. Comparison with the hot model: a scan of the parameter space

The main conclusion from this part of research is that neglecting the wavelength-dependence of radiation pressure, as in the classical hot model, produces an excess of local hydrogen density within ~ 10 AU from the Sun throughout the inner heliosphere except a cone region with the opening angle of $\sim 60^\circ$ around the downwind axis, as shown in Fig. 3 and 4. The excess density is a strong function of solar activity and while during solar minimum its typical values at 1 AU are about 40%, they are twice as big at solar maximum. At the downwind axis the hot model predicts a density deficit, which almost does not depend on the activity phase except at closest distances to the Sun. Discrepancies between the classical and Doppler models appear at ~ 10 AU and increase towards the Sun. Depending on the phase of the solar cycle and the offset angle from upwind, at 1 AU they reach from a few dozen percent up to a factor of ~ 1.8 .

This means that while at the distances of the maximum of the source function of the heliospheric backscatter glow in the upwind hemisphere the density computed with the use of the wavelength-insensitive model was overestimated only by $\sim 10\%$, the overestimation is much greater at the distances where in-situ measurements are carried out. Hence the absolute intensity of the helioglow is not heavily affected, but the density of the

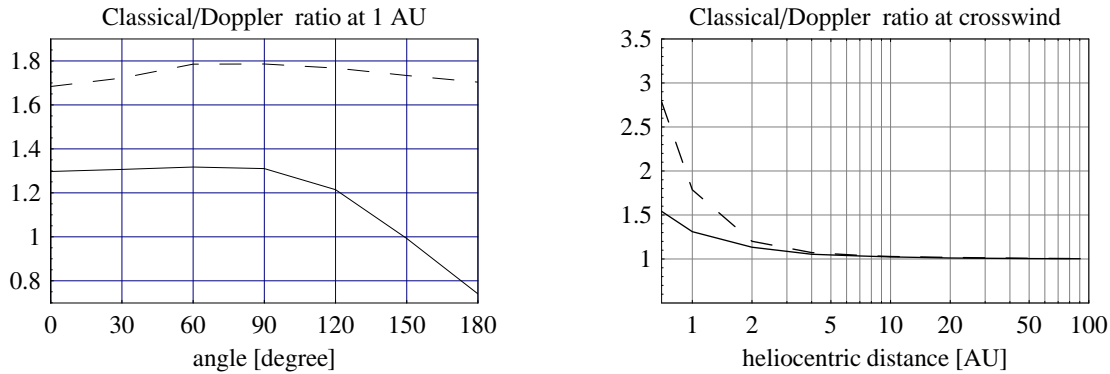


Fig. 3. Density excess of neutral interstellar hydrogen in the inner heliosphere, defined as a ratio of results of the classical hot model to the results of Doppler model. Left panel: density ratio at 1 AU as function of offset angle from the upwind direction, right panel: density ratio at crosswind as function of heliocentric distance. Solid lines correspond to solar minimum conditions, broken lines – to solar maximum conditions.

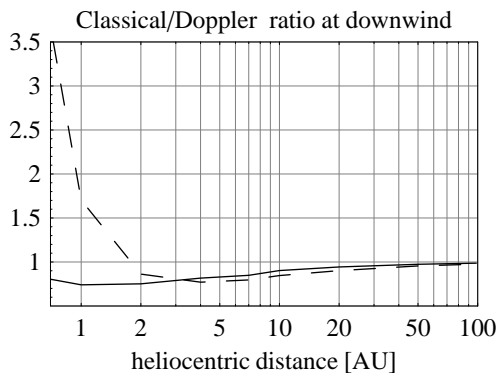


Fig. 4. Density ratio of the classical hot model to Doppler model at the downwind axis as function of heliocentric distance. Solid line: solar minimum conditions, broken line – solar maximum conditions.

gas inferred from observations of derivative populations such as Neutral Solar Wind and pickup ions, as well as planned in situ observations of interstellar H atoms by IBEX, interpreted with a wavelength-insensitive model, will be biased more heavily.

The existence of density excess can easily be understood after inspection of the shape of the solar Lyman- α line profile, shown in Fig. 1. Since the profile has a minimum close to the 0 radial velocity, the H atoms before approaching the Sun sense a stronger repulsion than in the case when one adopts a “flat” radiation pressure at the level of line center. Hence in the Doppler case a larger portion of these atoms will be repelled from the Sun, which reduces density in comparison with the classical case. The closer to the Sun one looks, the higher the “classical excess” is. In reality, the surviving ensemble of H atoms has a lower bulk velocity than predicted by the classical model, which leads to further enhancement of the excess because the ionization has more time to eliminate the atoms traveling with a smaller speed.

The magnitude of the excess is a weak function of temperature and bulk velocity of the atoms at the termination shock, as shown in Fig. 5.

Generally, the excess is consistently higher at a high activity period than at solar minimum, but one should keep in mind that the density at solar maximum is drastically reduced. The sensitivity of radiation pressure to radial velocity thus modifies the relations between densities during various phases of so-

lar activity (the amplitude of modulation), discussed, e.g., by Ruciński & Bzowski (1995b); Bzowski & Ruciński (1995a) and Bzowski et al. (2002).

The density excess is a weakly increasing function of the ionization rate (cf Fig. 6). This can be explained by preferential elimination of slower atoms from the local ensemble. As discussed by Bzowski et al. (1997), the result of ionization is a net acceleration of the gas by a few km/s because the atoms that have higher specific velocities are preferentially kept in the ensemble. Such atoms have also higher radial velocities and hence experience a higher radiation pressure due to the non-flat shape of the solar Lyman- α line profile. This force repels them from the Sun stronger than in the case when the solar line profile is flat. In the result we have a reduction of density – consequently, the classical model predicts an excess of density, whose magnitude increases with the increase of the ionization rate.

4.2. Realistic heliosphere

Having investigated the basic differences between the results of the Doppler model and the classical one and with the conclusions how they depend on the values of parameters such as the local ionization rate and bulk velocity and temperature at the termination shock, we can attempt to assess the influence of the non-flat shape of the solar Lyman- α line profile on a realistic heliosphere.

In this part of the paper we discuss composite populations of neutral interstellar atoms, made up of atoms belonging to the primary and secondary populations of interstellar H atoms, obtained from the classical and Doppler models (both with electron ionization included). The magnitude of the effects discussed should be representative for the realistic heliosphere, but must not be taken at face value because for the sake of clarity of the comparison we did not include the time evolution of the ionization rate and radiation pressure and the latitudinal anisotropy of these factors.

A global view of density excess/deficit returned by the classical model with respect to the Doppler code for solar minimum and maximum conditions is shown in Fig. 7. The simulations support the existence of density excess generated by the classical model for all offset angles from upwind except a cone with the opening angle $\sim \pm 30^\circ$ about the downwind axis. The excess increases towards the Sun both at solar minimum and maximum, but its magnitude changes by a factor of 2 from solar min. to solar max. During solar maximum the excess is predicted even

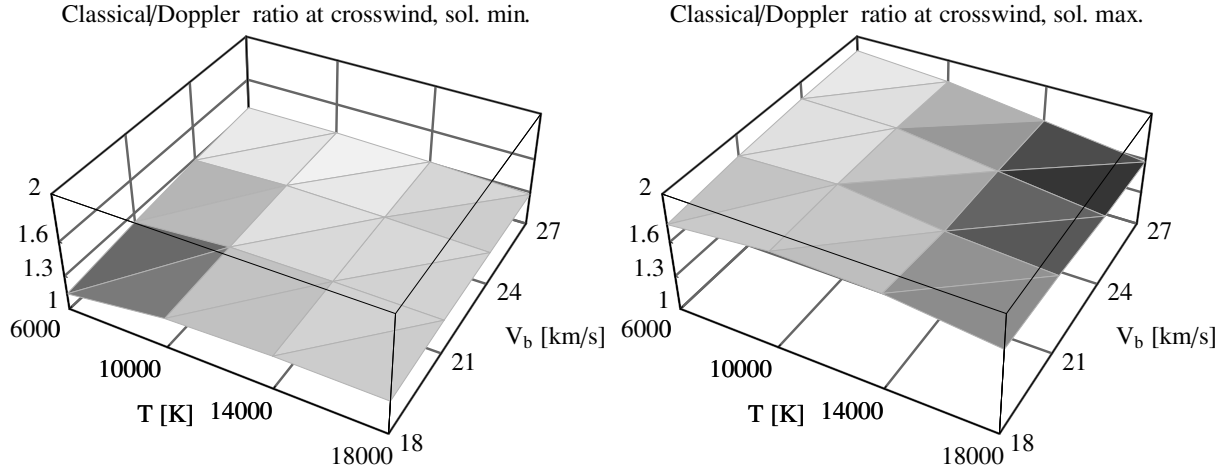


Fig. 5. Density excess of the classical hot model with respect to the Doppler model of neutral interstellar hydrogen as function of temperature and bulk speed in the source region for solar minimum (left panel) and solar maximum conditions (right panel).

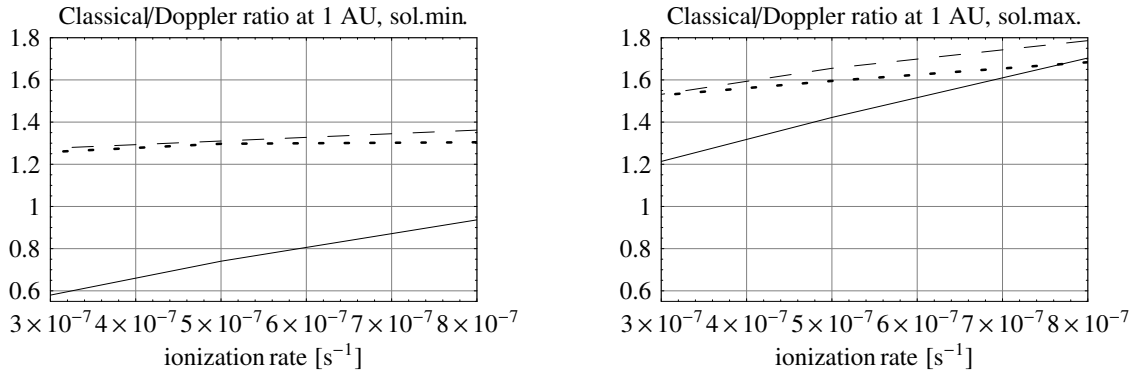


Fig. 6. Classical hot/Doppler model density ratios for the upwind (dots), crosswind (dashed) and downwind axes (solid) as function of the ionization rate for solar minimum (left panel) and maximum conditions (right panel).

in the downwind region, though only for distances smaller than ~ 2 AU.

The Doppler model predicts different ratios of densities between pairs of offset angles θ_1 , θ_2 (e.g. upwind/crosswind, upwind/downwind etc.) than the predictions of the classical hot model. The discrepancies are not strong in the upper hemisphere, but escalate with the increase of difference $\theta_2 - \theta_1$. This must be one of the reasons for which interpretation of downwind observations has always been more challenging than upwind and usually returned different conclusions. The challenge can be better appreciated when one realizes that the wavelength-sensitivity effects are convolved with the effects related to variations of solar Lyman- α flux and of the ionization rate, as discussed, e.g., by Ruciński & Bzowski (1995b); Bzowski & Ruciński (1995a,b).

The intensities of backscatter glow obtained from the Doppler and classical models – not surprisingly – agree to $\sim 10\%$. Discrepancies, however, are a monotonic function of the offset angle. The intensity excess visible at the upwind direction transforms into a similar deficit at the downwind axis (Fig. 8). The absolute magnitude of the effect is small and hence difficult to detect, but normalized profiles $I(\theta)/I(0)$ can vary by $\sim 15\%$. The amplitude of this effect is somewhat smaller than the amplitude of upwind-downwind temporal variations due to solar cycle variations of the radiation pressure and ionization rate, predicted by Ruciński & Bzowski (1995b), who show them at a $\sim 25\%$ level.

The Doppler model predicts also different local bulk velocities of the gas than the classical model (Fig. 12). Differences in radial component of the bulk velocity at 1 AU are on the order of a few km/s (Fig. 9). They start only at the offset angle $\theta \approx 60^\circ$ and increase towards downwind. The classical model systematically overestimates the radial velocity, which is easily understandable when one recalls that it notoriously underestimates the radiation pressure. Nevertheless, the differences in v_r are not big, so we do not expect big differences in model spectral profiles of the heliospheric glow.

The effect of the wavelength dependence of radiation pressure on the magnitude of fluxes of the two heliospheric neutral H populations is not negligible, though. As shown in Fig. 11, the difference between the results of Doppler and classical models is appreciable: at solar minimum the classical excess is 20 to 40%, depending on population, and during solar maximum it may reach a factor of 2, but with the absolute magnitude of the flux reduced by 2 orders of magnitude from the solar min. level (Fig. 10). In the upper hemisphere it is very weakly sensitive to the offset angle. The wavelength dependence of radiation pressure must then be appropriately taken into account in interpretation of direct in situ observations of neutral interstellar hydrogen atoms.

Another factor that potentially can affect interpretation of such measurements are differences in the local bulk velocity vectors of the two populations (Fig. 12). Möbius et al. (2001) pro-

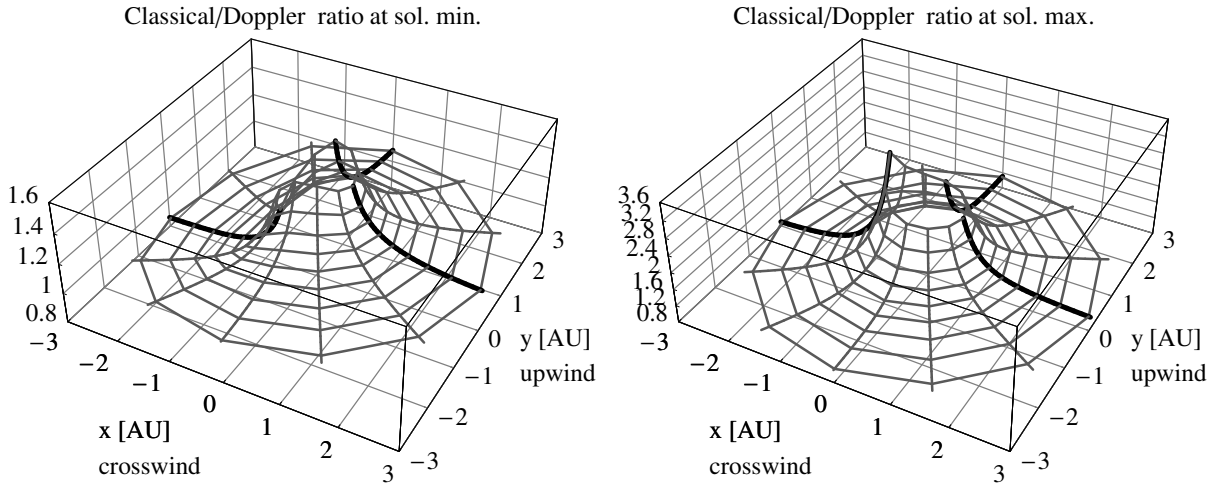


Fig. 7. Classical/Doppler composite density ratios for solar minimum (left panel) and solar maximum conditions (right panel). The Sun is at the center in the (0,0) point, the upwind – downwind direction is along the $y = 0$ line. The upwind, crosswind, and downwind axes are marked with heavy lines.

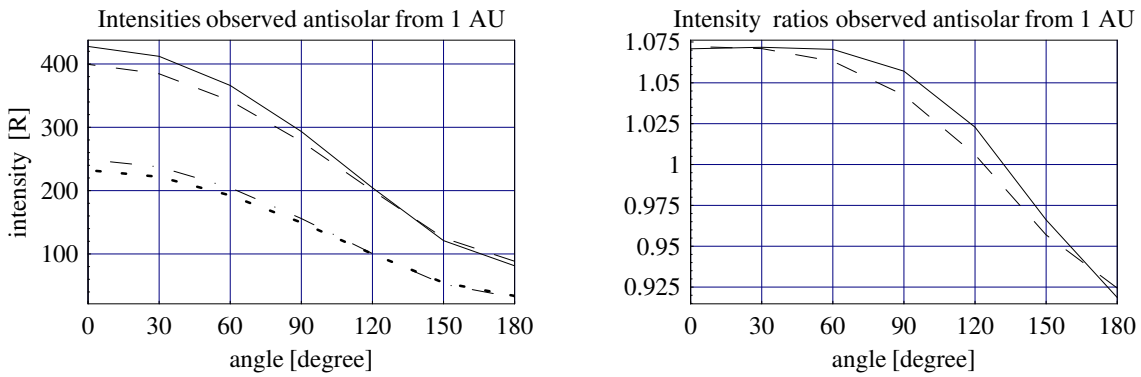


Fig. 8. Left panel: Absolute intensities of the heliospheric Lyman- α glow for solar maximum and minimum conditions, returned by the Doppler and classical hot models for antisolar lines of sight anchored at 1 AU from the Sun, as function of the offset angle from the upwind direction. The upper set of lines corresponds to solar minimum; the solid line is for the classical model, the broken line for Doppler model. The lower pair is for solar maximum and Doppler model is marked with dotted line, while the classical model by the dash-dot line. Right panel: classical/Doppler ratios of the intensities presented in the left panel; solid line corresponds to solar minimum, broken line to solar maximum. The intensities are calculated based on the composite gas densities obtained with the use of the Doppler and classical hot models, as discussed in text.

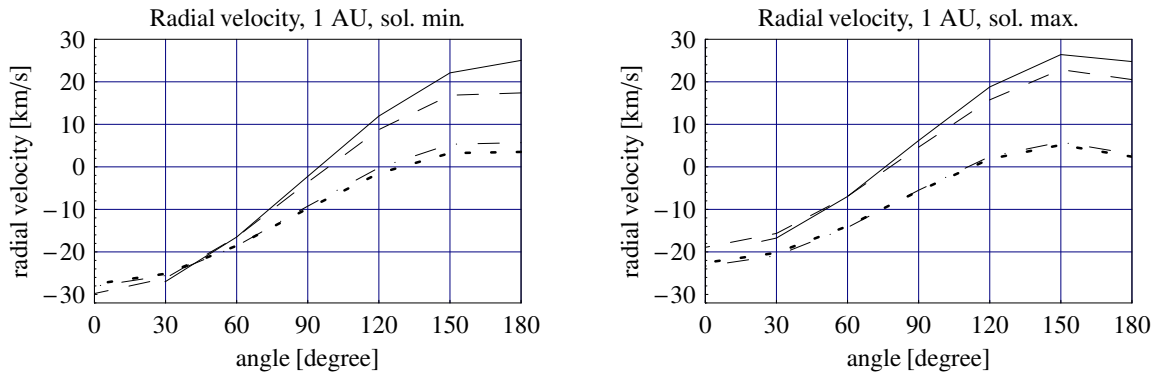


Fig. 9. Radial velocities of the primary and secondary populations of neutral H atoms at 1 AU as function of offset angle from upwind for solar minimum (left panel) and maximum conditions (right panel), calculated with the use of Doppler and classical hot model. The upper pairs of lines in both panels correspond to the primary population and the lower pairs to the secondary population. The classical hot model results are drawn, correspondingly, with solid and dash-dot lines, and the Doppler model results with broken and dotted lines.

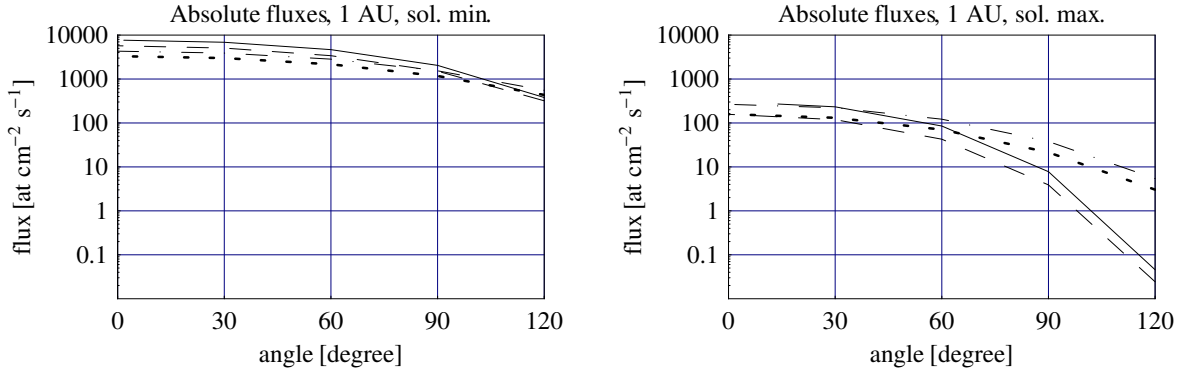


Fig. 10. Absolute fluxes of neutral interstellar H atoms at 1 AU from the primary and secondary populations for solar minimum (left panel) and solar maximum conditions (right panel), shown as function of the offset angle from upwind, calculated with the use of Doppler and classical hot models. The classical model results are drawn with solid line (primary populations) and dash-dotted line (secondary population); the Doppler model results with dashed (primary) and dotted lines (secondary).

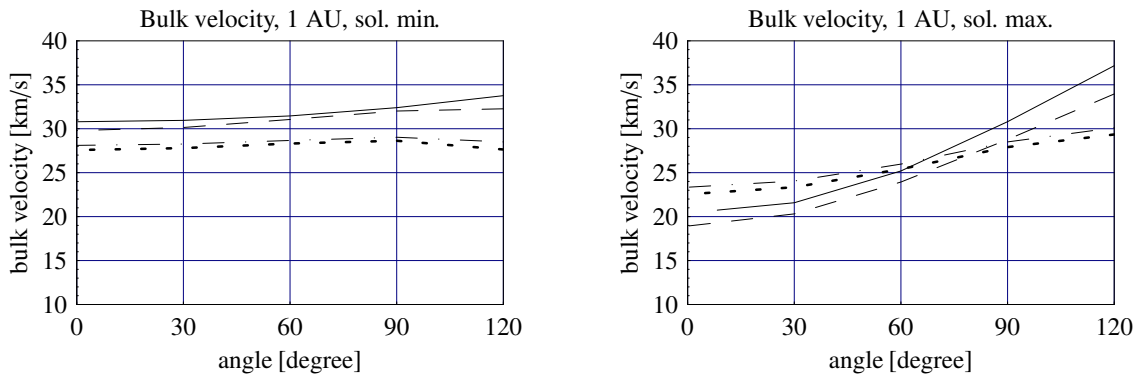


Fig. 12. Net bulk velocity of the primary and secondary populations of neutral interstellar H at 1 AU, calculated using the Doppler and classical hot models, shown as function of the offset angle from upwind for solar minimum (left panel) and solar maximum conditions (right panel). Primary population: solid line (classical) and broken line (Doppler); secondary population: dotted line (Doppler) and dash-dot (classical).

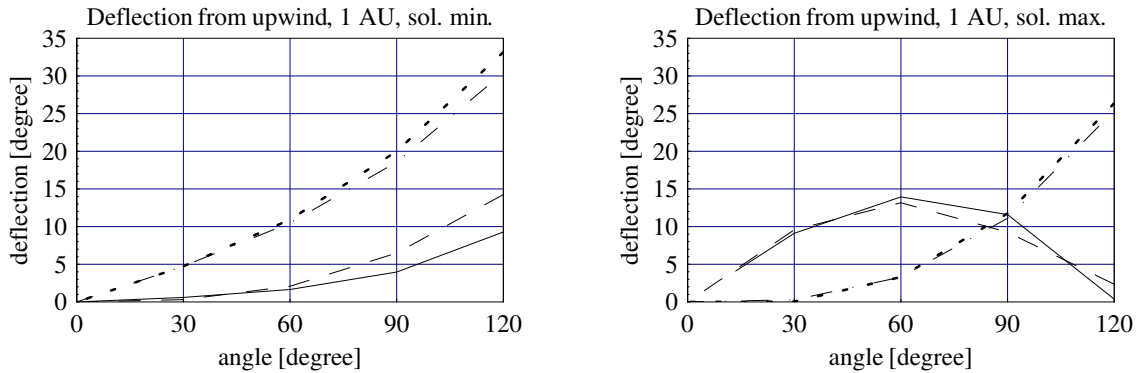


Fig. 13. Deflection of the local upstream direction of the primary and secondary population of interstellar hydrogen at 1 AU as function of offset angle from the gas inflow direction for solar minimum and maximum conditions. At solar minimum (left panel), less deflected is the primary population (solid line: classical model, broken line: Doppler model); the secondary is drawn with dotted line (Doppler) and dash-dotted line (classical). Same scheme for solar maximum plot (right panel).

posed to use the relative positions of the beams from the primary and secondary population to check whether their flow directions at the termination shock are parallel or not. Fig. 13 shows that in reality the deflections of the two populations will differ from the predictions of the wavelength-independent model and so will magnitudes of the local velocities. For both populations, in the region where detection is most probable owing to the advantageous geometry of the flow with respect to a spacecraft moving

with the Earth, the differences in deflection will be on the order of a few degrees, similar for both populations. The deflection is a strong function of solar activity, with radiation pressure clearly playing the dominant role in this respect. As could be expected, the deflection is stronger for the Doppler model.

Differences are predicted also for the net speed. They are at the level of ~ 2 km/s ($\sim 10\%$), which gives a $\sim 20\%$ difference in energy. They increase towards solar maximum.

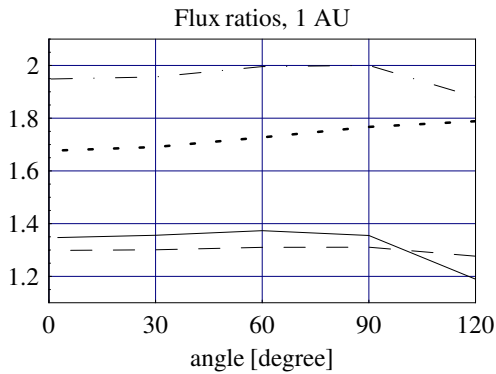


Fig. 11. Classical/Doppler ratios of the fluxes of primary and secondary populations of neutral interstellar H atoms for solar minimum and maximum as function of offset angle from upwind. The lower pair of the lines corresponds to solar minimum, the upper pair to solar maximum conditions. Within the solar minimum (lower) pair, the solid line corresponds to the primary population, the broken line to secondary population. Within the solar max. (upper) pair, the dash-dot line is for primary, the dotted line for secondary population.

Finally, we assess the influence of the wavelength-sensitive radiation pressure on the expected PUI fluxes at 5 AU crosswind (i.e., the location where the H^+ PUI flux observed by Ulysses is expected to be the strongest). This problem is discussed in greater detail by Bzowski et al. (2007, in preparation); here we only mention that the fluxes were computed following the simple classical approach by Vasyliunas & Siscoe (1976) and Gloeckler et al. (1993) and report that similarly as for all other aspects discussed before, the classical model yields an excess flux, which, however, is not big – at ~ 5 AU crosswind it is equal to only $\sim 7.5\%$ at solar minimum and to 8.5% at solar maximum. Thus we conclude that the actual flux should be about 10% lower than predicted by the classical model, irrespective of the solar activity phase.

5. Conclusions

1. Differences between the Doppler and classical hot models are restricted to ~ 10 AU from the Sun. The classical hot model overestimates the density of neutral hydrogen gas everywhere in the inner heliosphere except a $\sim 60^\circ$ cone around the downwind direction, where a density deficit is predicted. Generally, the density excess/deficit is a strong function of the offset angle from the upwind direction (Fig. 3 and 4).
2. The magnitude of density excess varies with the solar activity level and is higher at solar maximum (Fig. 7).
3. The density excess is a weak linear function of the ionization rate in the inner heliosphere and of the bulk velocity and temperature of the gas at the termination shock (Fig. 5 and 6).
4. Differences between the helioglow intensity observed antisolar from 1 AU, returned by the Doppler and classical models, are on the level of 10% and show a systematic behavior with the offset angle from upwind; this translates into a $\sim 30\%$ difference in the upwind/downwind ratios of intensities (Fig. 8).
5. The classical model shows a higher upwind-downwind amplitude of radial velocities at 1 AU than the Doppler model; the differences are on the order of 10%. The excess of abso-

lute flux of neutral atoms returned by the classical model are on the order of 30% at 1 AU during solar minimum, i.e. at the time of observations by the planned IBEX mission. The excess is much higher during solar minimum, but the absolute values of the fluxes are lower by a few orders of magnitude than during solar minimum (Fig. 9,10,11,12).

6. The classical model returns a different deflection of the local upstream directions of both heliospheric interstellar neutral H populations than the Doppler model. Hence interpretation of in situ measurements of these fluxes must be performed very carefully, with appropriate account for the solar line profile shape to avoid confusing deflections caused by the Doppler effect in radiation pressure with, e.g., results of deformation of the heliospheric interface due to external magnetic field (Fig. 13).
7. Discrepancies between the PUI flux at Ulysses in aphelion returned by the Doppler and classical models are on the order of 10% and are almost insensitive to the phase of solar cycle.

Acknowledgements. This work was supported by the Polish MSRI grant 1P03D00927.

References

- Axford, W. I. 1972, in *The Solar Wind*, ed. J. M. W. C. P. Sonnet, P. J. Coleman, NASA Spec. Publ. 308, 609
- Baranov, V. B., Lebedev, M. G., & Malama, Y. G. 1991, *ApJ*, 375, 347
- Baranov, V. B. & Malama, Y. G. 1993, *J. Geophys. Res.*, 98, 15157
- Bertaux, J. L. & Blamont, J. E. 1971, *A&A*, 11, 200
- Blum, P. & Fahr, H. J. 1970, *A&A*, 4, 280
- Bzowski, M., Fahr, H. J., Ruciński, D., & Scherer, H. 1997, *A&A*, 326, 396
- Bzowski, M. & Ruciński, D. 1995a, *Space Sci. Rev.*, 72, 467
- Bzowski, M. & Ruciński, D. 1995b, *Adv. Space Res.*, 16, 131
- Bzowski, M., Summanen, T., Ruciński, D., & Kyrölä, E. 2001, in *The outer heliosphere: the next frontiers*, ed. K. Scherer, H. Fichtner, H. J. Fahr, & E. Marsch, *COSPAR Colloquia Series Vol. 11* (Elsevier, Pergamon), 129–132
- Bzowski, M., Summanen, T., Ruciński, D., & Kyrölä, E. 2002, *J. Geophys. Res.*, 107, 10.1029/2001JA00141
- Chabrilat, S. & Kockarts, G. 1997, *Geophys. Res. Lett.*, 24, 2659
- Fahr, H. J. 1968, *Ap&SS*, 2, 474
- Fahr, H. J. 1978, *A&A*, 66, 103
- Fahr, H. J. 1979, *A&A*, 77, 101
- Fahr, H. J., Ripken, H. W., & Lay, G. 1981, *A&A*, 102, 359
- Gloeckler, G., Geiss, J., Balsiger, H., et al. 1993, *Science*, 261, 70
- Izmodenov, V., Malama, Y. G., Gloeckler, G., & Geiss, J. 2003, *ApJ*, 594, L59
- Izmodenov, V. V. 2000, *Ap&SS*, 274, 55
- Lemaire, P. L., Emerich, C., Vial, J. C., et al. 2002, in *ESA SP-508: From Solar Min to Max: Half a Solar Cycle with SOHO*, 219–222
- Malama, Y., Izmodenov, V. V., & Chalov, S. V. 2006, *A&A*, 445, 693
- Möbius, E., Litvinenko, Y., Saul, L., Bzowski, M., & Ruciński, D. 2001, in *The Outer Heliosphere: The Next Frontiers*, ed. K. Scherer, H. Fichtner, H. J. Fahr, & E. Marsch, *COSPAR Colloquia Series Vol. 11* (Elsevier, Pergamon), 69–72
- Ruciński, D. & Bzowski, M. 1995a, *A&A*, 296, 248
- Ruciński, D. & Bzowski, M. 1995b, *Adv. Space Res.*, 16, 121
- Ruciński, D. & Bzowski, M. 1996, *Space Sci. Rev.*, 78, 248
- Ruciński, D. & Fahr, H. J. 1989, *A&A*, 224, 290
- Ruciński, D. & Fahr, H. J. 1991, *Annales Geophys.*, 9, 102
- Scherer, H., Bzowski, M., Fahr, H. J., & Ruciński, D. 1999, *A&A*, 342, 601
- Thomas, G. E. 1978, *Ann. Rev. Earth Planet. Sci.*, 6, 173
- Thomas, G. E. & Krassa, R. F. 1971, *A&A*, 11, 218
- Tobiska, W. K., Woods, T., Eparvier, F., et al. 2000, *J. Atm. Terr. Phys.*, 62, 1233
- Vasyliunas, V. & Siscoe, G. 1976, *J. Geophys. Res.*, 81, 1247
- Vidal-Madjar, A. 1975, *Sol. Phys.*, 40, 69
- Wilhelm, K., Woods, T. N., Schühle, U., et al. 1999, *A&A*, 352, 321
- Wu, F. M. & Judge, D. L. 1979, *ApJ*, 231, 594